Photodiagnosis and Photodynamic Therapy 40 (2022) 103090

Contents lists available at ScienceDirect

Photodiagnosis and Photodynamic Therapy

journal homepage: www.elsevier.com/locate/pdpdt

Intracellular glutathione levels affect the outcomes of verteporfin-mediated photodynamic therapy in esophageal cancer cells

Mirai Edano, Tsutomu Kanda *, Ryohei Tarumoto, Wataru Hamamoto, Takashi Hasegawa, Yukari Mae, Takumi Onoyama, Tomoaki Takata, Takaaki Sugihara, Hajime Isomoto

Division of Gastroenterology and Nephrology, Faculty of Medicine Tottori University, 36-1 Nishi-Cho, Yonago, Tottori, Japan

ARTICLE INFO

Keywords:
Esophageal cancer
Verteporfin
Photodynamic therapy
Glutathione
Sulfasalazine

ABSTRACT

Photodynamic therapy (PDT) induces cancer cell death by generating reactive oxygen species (ROS). In this process, photosensitizers accumulate in cancer cells irradiated by laser light of a specific wavelength, leading to ROS generation. Verteporfin (VP), a second-generation photosensitizer, is used in PDT for age-related macular degeneration. However, the antitumor effects of VP-PDT remain poorly defined. This study investigated the antitumor effects of VP-PDT on esophageal cancer (EC) cell lines *in vitro*. Two types of EC cell lines, the KYSE30 cell line, derived from highly differentiated esophageal carcinoma, and the KYSE170 cell line, derived from moderately differentiated carcinoma, were used in this study. VP-PDT exerted effective anticancer effects in both cell lines. Our results revealed that the low-density lipoprotein receptor, albumin receptor, and heme carrier protein-1 in VP uptake were not involved in VP uptake. However, cells rich in intracellular glutathione were resistant to VP-PDT. Our study outcomes suggest that lowering intracellular glutathione via a glutathione synthesis inhibitor or sulfasalazine can increase the effectiveness of VP-PDT-mediated anticancer effects.

1. Introduction

Esophageal cancer (EC) is one of the leading causes of cancer-related deaths worldwide [1]. Depending on the disease stage, EC patients are subjected to endoscopic treatment, surgical treatment, chemotherapy, or radiation therapy [2]. In addition to these conventional treatment strategies, photodynamic therapy (PDT), using talaporfin sodium (TS), has been approved and is currently being used in Japan for residual or recurrent EC after radiation therapy or chemoradiation. PDT is a minimally invasive treatment with fewer side effects [1] than endoscopic resections, and its technical quality can be calibrated more efficiently.

In PDT, a photosensitizer is administered that accumulates in cancer cells, and upon irradiation with a specific wavelength of laser, generates reactive oxygen species (ROS), thereby, inducing cell death [3]. The photosensitizer can specifically accumulate in tumors, and local irradiation can selectively treat tumor lesions. When irradiated with a specific wavelength, photosensitizer is excited from the ground (S0) to the singlet (S1) state. Thereafter, the photosensitizer enters the triplet state (S3) due to intersystem crossing and returns to S0 while providing energy to oxygen molecules, which reach S1 and destroy cancer cells [3].

In Japan, the first-generation photosensitizer, porfimer sodium (PS), and second-generation photosensitizers, TS and verteporfin (VP), have been approved for PDT. However, to avoid post-treatment sunlight sensitivity, PS-based PDT requires a light-blocking period of 4 weeks, whereas the second-generation photosensitizer, TS, requires a continuous light-blocking period of at least 2 weeks. In contrast, VP-based PDT requires a light-blocking period of no more than 2 days, which is considerably shorter compared with that for PS and TS. As VP-based PDT has well-established effectiveness and safety, it is widely used to treat age-related macular degeneration [4,5].

The absorption peak of VP is at 689 nm, whereas those of PS and TS are at 630 and 664 nm, respectively. The longer-wavelength light (689 nm) penetrates more deeply and can treat more invasive EC. In addition, clinical trials of VP-PDT for locally advanced pancreatic cancer have confirmed its antitumor effects and safety [5].

We previously showed that the expression of the low-density lipoprotein (LDL) receptor determines the efficacy of TS-PDT [6]. We investigated the involvement of LDL receptors [6,7], albumin receptors [8], and heme carrier protein (HCP)-1 to determine PDT efficacy [9].

Saya et al. showed that glutathione removes the ROS in cancer stem cells and, hence, is a potential factor in treating ROS-related cancer resistance mechanism [10], which works as follows: variants of CD44,

* Corresponding author.
E-mail address: tsutomu-k@tottori-u.ac.jp (T. Kanda).

https://doi.org/10.1016/j.pdpdt.2022.103090
Received 26 March 2022; Received in revised form 9 August 2022; Accepted 23 August 2022
Available online 27 August 2022

which is an important cancer stem cell marker, stabilize cystine transporters on the cell surface and enhance cystine uptake; the increased cystine content enhances glutathione synthesis as cystine is one of the constituent amino acids in glutathione [10]. Saya et al. reported that sulfasalazine (SASP) inhibits the growth of CD44 variant 9 (CD44v9)-positive cancer stem cells [11]. Moreover, Timmerman et al. reported that the amino acid transporter, xCT, is the target of SASP [12]. SASP is a therapeutic drug for rheumatoid arthritis and ulcerative colitis. ROS-mediated cancer cell resistance has been evaluated using hydrogen peroxide. However, to date, the mechanism of ROS-mediated resistance due to singlet oxygen generated by PDT has not been evaluated.

Unlike TS-PDT, VP-PDT is not currently indicated for EC. We, therefore, conducted a preliminary study to expand its indication for EC. In this study, we investigated the antitumor effect of VP-PDT on two types of EC cell lines—KYSE30, derived from highly differentiated carcinoma, and KYSE170, derived from moderately differentiated carcinoma—*in vitro* based on the determination of EC_{50}, and evaluated its potential for future clinical implementation. Because the chemical structure of VP is very similar to that of TS (Supplementary Fig. 1), we expected that the same receptors as those of TS would affect the uptake of VP. Therefore, we compared the expression levels of the above-mentioned receptors. Moreover, the amount of intracellular glutathione, and the effect of SASP on VP-PDT in EC cell lines were investigated.

2. Materials and methods

2.1. Human EC cell lines and culture

The EC cell lines, KYSE30 and KYSE170, were obtained from the JCRB Cell Bank (Osaka, Japan). KYSE30 cells were cultured in Dulbecco's modified Eagle medium supplemented with 2% fetal bovine serum. KYSE170 cells were cultured in RPMI-1640/Nutrient Mixture F-12 medium supplemented with 2% fetal bovine serum. All cell culture media were supplemented with 2 mM L-glutamine solution without antibiotics. The cells were cultured in a humidified incubator with 5% CO_2 at 37°C.

2.2. Reagents

Verteporfin (VP, SML0534) and sulfasalazine (SASP, S0883) were purchased from Merck KGaA (Darmstadt, Germany). The MitoBright Green (MT06) was purchased from the Dojindo Laboratories, Co., Ltd. (Kumamoto, Japan). For cell staining, crystal violet (031-04852) was purchased from Fujifilm Wako Pure Chemical Co., Ltd. (Osaka, Japan). The GSH-Glo™ Glutathione Assay (V6911) and CellTiter 96® AQueous One Solution Cell Proliferation Assay (G3580) kits were purchased from Promega Co. (Tokyo, Japan). To inhibit glutathione synthesis, L-buthionine-(S, R)-sulfoximine (BSO, 14484) was purchased from Cayman Chemical Co. (Ann Arbor, MI, USA). Accutase (AT104, Innovative Cell Technologies, Inc., San Diego, CA, USA), rabbit monoclonal antibody against LDL receptor (ab52818, Abcam PLC., Tokyo, Japan), rabbit polyclonal antibody against HCP1/PCFT (ab25134, Abcam PLC), rabbit polyclonal antibody against SPARC (ab55847, Abcam PLC.) as albumin receptor, rat monoclonal antibody against CD44 variant 9 (CD44v9) (LKG-M003, COSMO BIO Co., LTD., Tokyo, Japan), rabbit monoclonal antibody against β-actin (D6A8) (8457, CST Japan Co., Ltd.), goat anti-rabbit IgG H&L conjugated to horseradish peroxidase (HRP) (ab97051, Abcam PLC.), and goat anti-rat IgG H&L (HRP) (ab97057, Abcam PLC) were purchased for western blotting analysis.

2.3. PDT protocol and crystal violet staining

Cells were treated with VP in a serum-free medium for 15 min in the dark and then irradiated with a 689 nm LED at 3 or 10 J/cm^2. After 24 h, cells were fixed with 4% paraformaldehyde for 5 min at 20–25°C, stained with 0.05% crystal violet for 30 min at 20–25°C, washed with phosphate-buffered saline (PBS), and dried. After imaging, methanol was added to dissolve the dye, and the absorbance was measured at 540 nm using a microplate reader (Vientonano; DS Pharma Biochemical Co., Ltd.) to evaluate the viability of cancer cell lines after VP-PDT and the half-maximum effective concentration (EC_{50}) value of VP was calculated.

2.4. Microscopic imaging

Cells were visualized with a fluorescence microscope (BZ-X710; Keyence Co., Osaka, Japan) using the BZ-X filter GFP (OP-87763; Keyence Co.). To visualize the VP, a filter cube (OP-87767; Keyence Co.) was used with relevant excitation (405BP20) and fluorescence (RPE630LP) filters. The software BZ-analyzer (Ver.1.3.1.1., Keyence Co.) was used to merge, reduce noise, and enhance the signal intensity.

2.5. Fluorescent staining of intracellular organelles

We observed that VP had a porphyrin structure and emitted red light when the excitation irradiation was 405 nm. Cells were incubated with 0.1 μM VP for 1–20 min at 37°C in the dark. After washing with PBS twice, cells were exposed to 0.1 μM MitoBright Green (10 min, 20–25°C). This stain accumulates in the mitochondria of live cells based on the mitochondrial membrane potential. After washing with PBS, cells were imaged under a fluorescence microscope (BZ-X710, Keyence Co.).

2.6. Western blot analysis

Cultured cells were lysed for 15 min on ice with RIPA buffer (182-02451, Fujifilm Wako Pure Chemical Co., Ltd.) containing cOmplete™ ULTRA Tablets, mini, EASYpack Protease Inhibitor Cocktail, and PhoSTOP (05892970001 and 4906845001, Roche Diagnostics Co., Ltd., Tokyo, Japan). To harvest CD44v9, we used Accutase, a mild cell dispersion solution, before treatment with the RIPA buffer. After centrifugation at 21,500 × *g* for 15 min, protein concentrations were measured using Pierce 660 nm Protein Assay Reagent (1861426, Thermo Fisher Scientific Inc., Tokyo, Japan). Proteins were denatured by boiling for 5 min or at 70°C for 10 min (for detection of HCP-1) with or without 2-mercaptoethanol (for detection of CD44v9). Equal amounts of protein samples (30 μg) were subjected to SDS-PAGE and then transferred onto nitrocellulose or polyvinylidene fluoride (1215471, GVS) (for detection of CD44v9) membranes. After blocking with 5% milk in TBST (150 mmol/L NaCl and 50 mmol/L Tris-HCl, containing 0.05% Tween-20), membranes were incubated with anti-LDL receptor antibody (dilution, 1:1000), anti-HCP-1 antibody (dilution, 1:500), anti-SPARC antibody (dilution, 1:1000), anti-CD44v9 antibody (dilution, 1:500), and anti-β-actin antibody (dilution, 1:10,000) at 4°C overnight. After three washes with TBST (5 min each), the membranes were incubated with their corresponding HRP-conjugated secondary antibodies (dilution, 1:5000) for 1 h at 20–25°C. After three washes with TBST (5 min each), the signal was visualized using the Clarity Western ECL Substrate (1705061, Bio-Rad Laboratories, Inc., Tokyo, Japan) and image analyzer (LAS-3000 mini, Fujifilm Co. Ltd., Tokyo, Japan).

2.7. RNA extraction

Total RNA was extracted from cultured cells using a miRNeasy Mini Kit (217004; QIAGEN Co., Ltd., Tokyo, Japan). The extracted RNA was quantified using a BioSpec-nano spectrophotometer (206-26300-41; Shimadzu Co., Ltd., Kyoto, Japan). The extracted RNA samples were stored at −80°C until further use.

2.8. Quantitative PCR

cDNA was prepared from total RNA using a High-Capacity cDNA Reverse Transcription Kit (4374966, Thermo Fisher Scientific Inc., Tokyo, Japan). The reverse transcription reactions were performed in

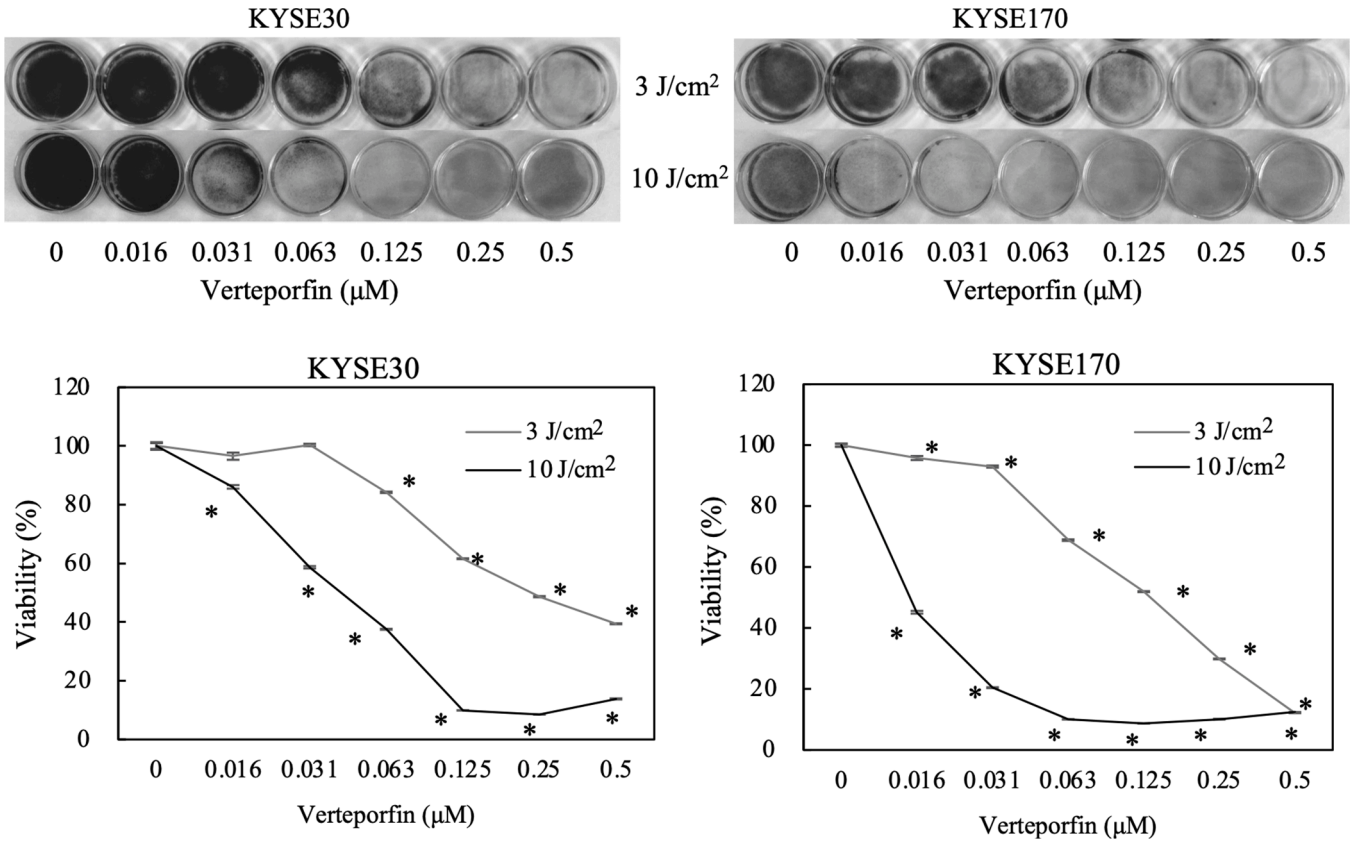

Fig. 1. Crystal violet staining after VP-PDT (689 nm, 3 J/cm^2, or 10 J/cm^2), followed by optical measurement and quantification. VP, verteporfin. PDT and photodynamic therapy.

aliquots containing 2000 ng total RNA, 1 × RT buffer, 4 mM dNTP mix, 1 × RT random primer, 50 units Multi-Scribe reverse transcriptase, and 20 units RNase inhibitor; nuclease-free water was added up to 20 μL. For reverse transcription, reaction mixtures were incubated at 25°C for 10 min, and subsequently at 37°C for 120 min and at 85°C for 5 min. The primer sequences for quantitative PCR were as follows: *LDL receptor* forward: 5′- TCTGCAACATGGCTAGAGACT-3′, reverse: 5′-TCCAAGCATTCGTTGGTCCC-3′; *SPARC* (*albumin receptor*) forward: 5′-TGAGGTATCTGTGGGAGCTAATC-3′, reverse: 5′-CCTTGCCGTGTTTGCAGTG-3′; *HCP-1* forward: 5′-AGAGCTGGACAATGGATCGGT-3′, reverse: 5′-GCCTTGCTGATAGCCATGACTC-3′; *CD44v9* forward: 5′-GGCTTGGAAGAAGATAAAGACC-3′, reverse: 5′-TGCTTGATGTCAGAGTAGAAGTTG-3′; and *β-actin* forward: 5′-CATGTACGTTGCTATCCAGGC-3′, reverse: 5′-CTCCTTAATGTCACGCACGAT-3′. The quantitative PCR was performed in 20 μL aliquots containing 1 μL RT products, 4 μL LightCycler® Fast-Start DNA MasterPLUS SYBR Green I (03515869001, Roche Diagnostics Co., Ltd., Tokyo, Japan), 0.5 μM each primer, and 14.6 μL nuclease-free water, and run on the Real-Time PCR LightCycler 1.5 Complete System (Roche Diagnostics Co., Ltd., Tokyo, Japan). The thermal cycling was initiated with a first denaturation step at 95°C for 10 min, followed by 45 cycles of 95°C for 10 s, 60°C for 10 s, and 72°C for 10 s. The threshold cycle (C_t) values were recorded using LightCycler software version 3.5.28 (Roche Diagnostics Co., Ltd., Tokyo, Japan), and *β-actin* was used as the endogenous control for data normalization. Relative expression was calculated using the formula $2^{-\Delta\Delta Ct} = 2^{-}$ (ΔCt, reagent treatment - ΔCt, control) [13].

2.9. Hydrogen peroxide treatment

The cells were treated with 0.5 mM H_2O_2 in a serum-free medium for 30 min at 37°C, and cell viability was measured using the MTS (3-(4,5-dimethylthiazol-2-yl)-5-(3-carboxymethoxyphenyl)-2-(4-sulfophenyl)-2H-tetrazolium) assay.

2.10. Preparation of the SASP stock solution

The SASP powder was dissolved in 0.1N NaOH, adjusted to a concentration of 20 mM in PBS, and the pH was adjusted to 7.2–7.6 using 1N HCl. When used, the stock solution was diluted with the culture medium.

2.11. BSO and SASP treatment

Cells were treated with BSO or SASP diluted in the culture medium for 24 h at 37°C, and the intracellular glutathione content and cell viability were measured using the GSH-Glo glutathione assay and MTS assay, respectively.

2.12. GSH-Glo glutathione and the MTS assays

KYSE30 and KYSE170 cells were seeded at 5000 and 2500 cells/well in 96-well flat, clear plates, respectively. For glutathione detection, cells were washed with PBS and 100 μL reaction buffer containing luciferin-NT substrate, and glutathione S-transferase was added to each well. Subsequently, cells were incubated in the dark for 30 min at 20–25°C. Next, 100 μL detection buffer was added, and cells were incubated in the dark for 15 min at 20–25°C. Finally, the fluorescence intensity was measured using a microplate reader (Infinite F500; Tecan Japan Co., Ltd.; Kanagawa, Japan). The cell viability was measured using the MTS assay, which was performed as follows: 20 μL proliferation assay solution was added to 100 μL culture medium, and after 1 h, the absorbance was measured at 490 nm using a microplate reader (Vientonano, DS Pharma Biochemical Co., Ltd., Osaka, Japan). Finally, the amount of intracellular glutathione was corrected, and viability was assessed

Table 1
EC_{50} of VP after VP-PDT (689 nm, 3 J/cm^2 or 10 J/cm^2). VP, verteporfin. PDT, photodynamic therapy.

EC50 values of VP.		
	EC50 of VP (μM)	
	KYSE30	KYSE170
3 J/cm^2	0.22	0.05
10 J/cm^2	0.16	0.02

[i] EC50, half maximal effective concentration; VP, verteporfin.

against that of control cells.

2.13. Statistical analysis

The differences between the VP-PDT and control groups were analyzed using the paired two-tailed Student's *t*-test. Differences among the three groups were analyzed using Tukey's test after a one-way or two-way ANOVA. Data are expressed as mean ± standard deviation. The differences were considered statistically significant at $p < 0.05$.

3. Results

3.1. EC_{50} of VP-PDT in EC cell lines

VP-PDT exerted cytotoxic effects in both the EC cell lines (Fig. 1). The effect was dependent on the VP dose and light intensity (Fig. 1). In KYSE30 cells, the EC_{50} values upon VP treatment followed by iradiation at 3 and 10 J/cm^2 were 0.22 and 0.16 μM, respectively, whereas the values were 0.05 and 0.02 μM, respectively, for KYSE170 cells (Table 1).

3.2. Expression of receptors

As shown in Fig. 2, the mRNA expression of the three receptors differed significantly between KYSE30 and KYSE170 cells. The level of LDL receptor was higher in KYSE30 cells than in KYSE170 cells. The albumin receptor and HCP-1 were overexpressed in KYSE170 cells compared with that in KYSE30 cells. However, the expression of these receptors was not significantly different at the protein level.

3.3. Verteporfin uptake and localization

As shown in Fig. 3, the amount of accumulated VP and its uptake rate did not differ between 1 and 15 min of treatment. In addition, we considered the possibility that VP is localized in the mitochondria of both cell lines.

3.4. Resistance to oxidative stress and intracellular glutathione levels

The sensitivity to hydrogen peroxide was significantly higher in KYSE170 cells than in KYSE30 cells (Fig. 4A). Intracellular glutathione levels were significantly higher in KYSE30 cells than in KYSE170 cells (Fig. 4B). The protein and mRNA expression of the CD44 variant 9 (CD44v9) were higher in KYSE30 cells than in KYSE170 cells (Fig. 4C and 4D).

3.5. Cytotoxic effects of BSO

Cytotoxic effects were not observed upon treating either cell line with 10 and 100 μM BSO (Fig. 5A). The BSO treatment (10 or 100 μM) decreased intracellular glutathione levels in both the cell lines (Fig. 5B). The efficacy of VP-PDT was enhanced in response to 10 and 100 μM BSO treatment in KYSE30 cells and by 10 μM BSO treatment in KYSE170 cells (Fig. 5C). In KYSE30 cells, the effect of BSO was observed at both 0.1 and 0.2 μM VP, whereas in KYSE170 cells, the effect of BSO was observed at 0.025 μM VP, but not at 0.05 μM VP.

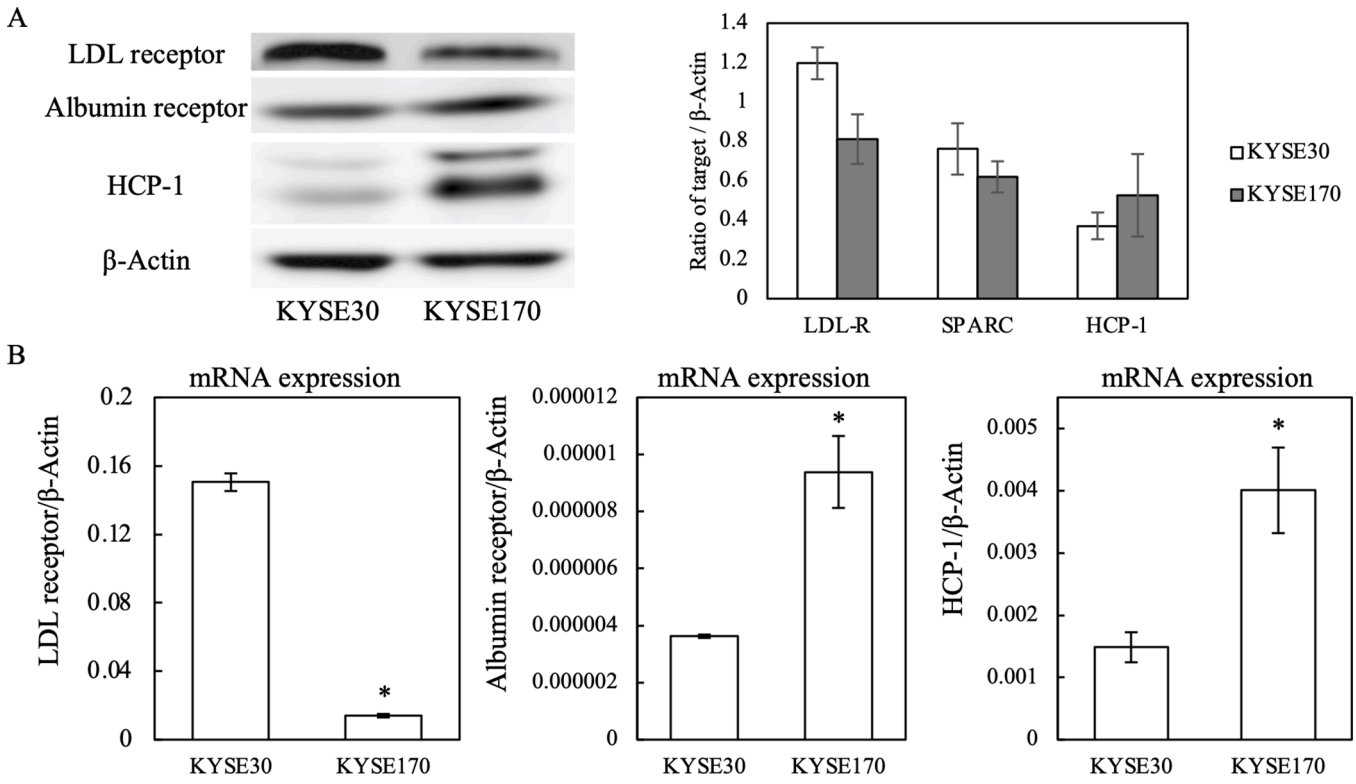

Fig. 2. Expression of the LDL receptor, albumin receptor, HCP-1, and β-actin on the KYSE30 and KYSE170 cells. (A) The protein was measured by western blotting. (B) mRNA level measured by RT-PCR. *p < 0.05 vs. each control (n = 4). Error bar represents the standard deviation. LDL, low-density lipoprotein. HCP, heme carrier protein.

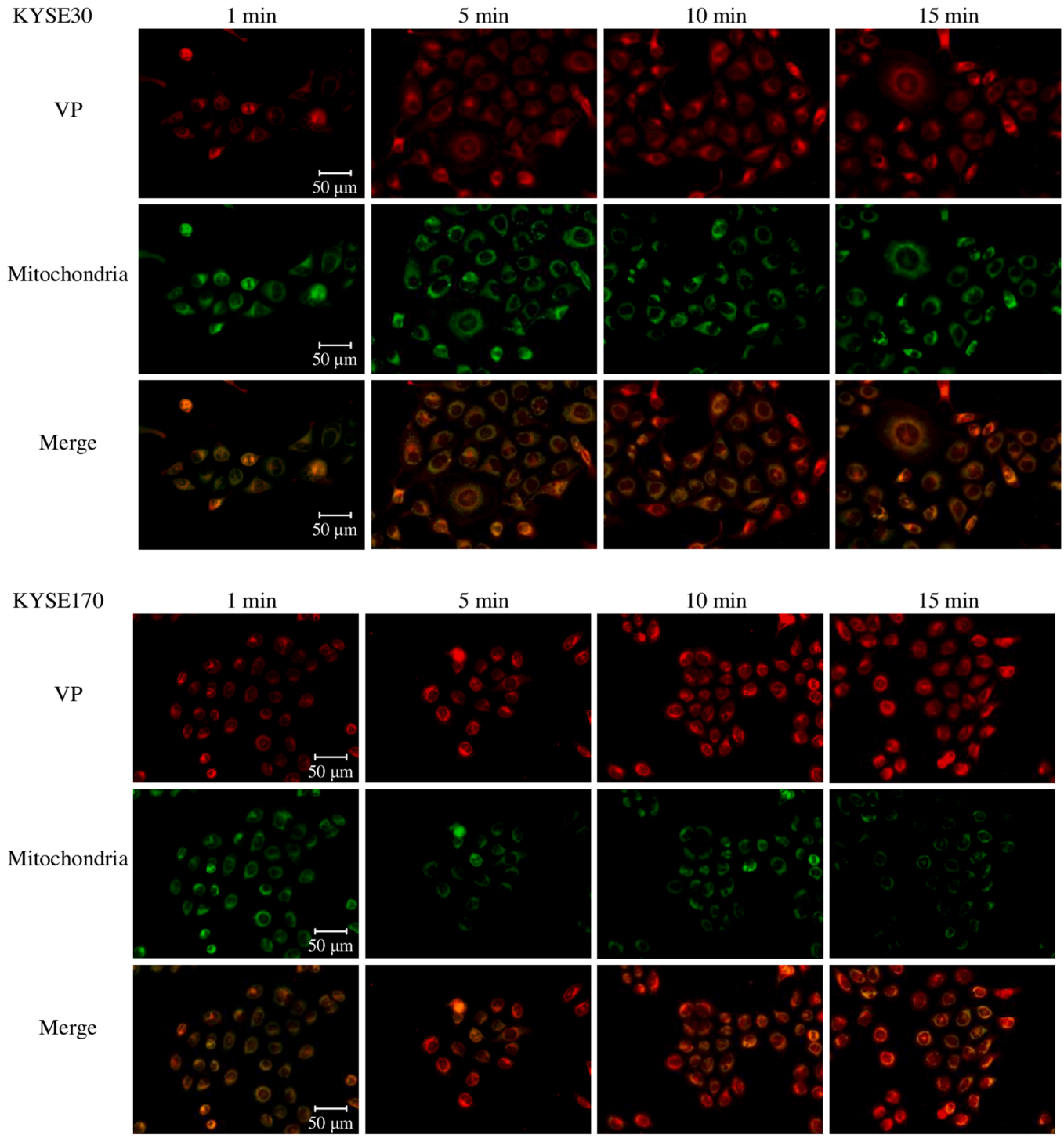

Fig. 3. VP uptake and localization in KYSE30 and KYSE170 cells. The VP positive region is stained red, and mitochondria are stained green (objective lens, × 10). After 0.1 μM VP treatment, the fluorescence intensity was observed at the intervals of 1, 5, 10, and 15 min. VP, verteporfin.

3.6. SASP effects

Cytotoxic effects of SASP (0.25 and 0.5 mM SASP) were observed in KYSE30 and KYSE170 cells (Fig. 6A). Upon SASP treatment (>0.25 mM), the intracellular glutathione decreased in both cell lines (Fig. 6B). In KYSE30 cells, the SASP treatment enhanced the efficacy of VP-PDT at 0.25 and 0.5 mM; however, it was effective only at 0.5 mM in KYSE170 cells (Fig. 6C).

4. Discussion

Our results show that the VP-PDT is effective in both KYSE30 and KYSE170 cell lines, although their sensitivity differs. The EC_{50} of VP-PDT (Table 1) was less than 1/6 of the maximum blood concentration (1.84 μM) used in the treatment of age-related macular degeneration (see the package insert for Visudyne). This EC_{50} was also lower than that reported by Mae et al. when VP-PDT was performed on gastric cancer cell lines [14]. This could be attributed to the use of LEDs at 689 nm in our study, which is the peak of the absorption coefficient of VP,

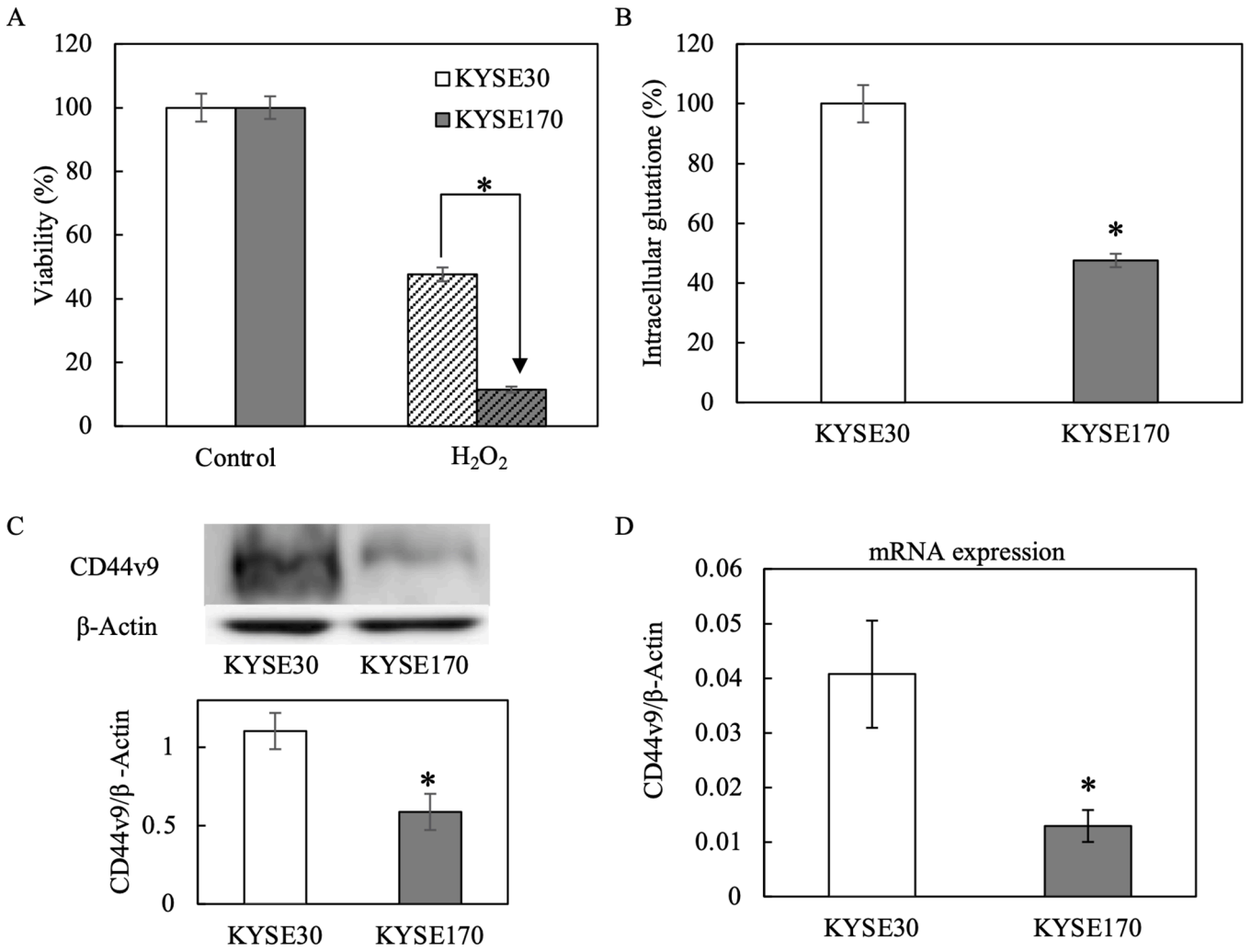

Fig. 4. (A) Resistance to oxidative stress. KYSE30 and KYSE170 cells were treated with 0.5 mM H_2O_2 for 30 min, and the viability was measured by the MTS assay. (B) Intracellular glutathione was measured by the GSH-Glo glutathione assay. (C) CD44v9 protein level was measured by western blotting. (D) *CD44v9* mRNA was measured by RT-PCR. *$p < 0.05$ vs. each control ($n = 4$). The error bar represents the standard deviation. CD44v9, CD44 variant 9.

compared with 660 nm LEDs used in the previous study [14].

We evaluated the expression of three receptors—LDL receptor, albumin receptor, and HCP-1. These receptors were selected because the structure of VP is similar to that of talaporfin sodium (Supplementary Fig. 1). The expression of these receptors differed between KYSE30 and KYSE170 cells at the mRNA level but not at the protein level (Fig. 2). Moreover, there was no difference in the amount and speed of VP uptake, and in its localization (Fig. 3). Therefore, we believe that VP uptake is not related to the EC_{50}, and there might be other reasons for it, such as the presence of intracellular antioxidants.

The sensitivities of both the cell lines to oxidative stress and hydrogen peroxide differed (Fig. 4A). Additionally, the amount of the intracellular glutathione content varied (Fig. 4B), and CD44v9 was differentially expressed (Fig. 4C and 4D). Saya et al. reported that the CD44 variant induces resistance to ROS via upregulating the cysteine uptake, an amino acid component of glutathione [10]. Therefore, we propose that the differential expression of CD44v9 increased the intracellular glutathione content, thereby, helping these cells to acquire resistance to oxidative stress.

The glutathione synthesis inhibitor, BSO, did not show cytotoxicity in our study (Fig. 5A); however, it decreased the intracellular glutathione levels (Fig. 5B) in KYSE30 and KYSE170 cells. Although BSO enhanced the efficacy of VP-PDT in both cell types, the effect was weak (Fig. 5C). KYSE170 cells are intrinsically more sensitive to VP-PDT than KYSE30 cells. Therefore, we believe that at 0.05 μM VP, VP-PDT alone is sufficiently effective so that BSO seems to exert no effect. We speculate that factors other than intracellular glutathione level regulate this phenomenon, although they remain currently unknown.

Because BSO has not been approved for the clinical setting, we evaluated the effects of SASP in our experimental model. SASP has been approved as a therapeutic drug for rheumatoid arthritis and ulcerative colitis. Additionally, SASP exerts antiproliferative effects on cancer cells [11] by targeting xCT, a cystine-glutamate transporter [12]. SASP exerted cytotoxic effects (Fig. 6A) and decreased the intracellular glutathione content corrected for cell number (Fig. 6B) in KYSE30 and KYSE170 cells. In both the cell lines, the SASP treatment enhanced the efficacy of VP-PDT. Moreover, treatment with 0.25 mM SASP appeared to have a synergistic effect in KYSE30 cells (Fig. 6C). However, 0.5 mM SASP had an additive effect in KYSE30 and KYSE170 cells (Fig. 6C). Furthermore, in PDT using TS, SASP treatment enhanced the efficacy in an additive manner (Supplementary Fig. 2). Our results show a definite positive effect of SASP treatment in enhancing the efficacy of VP-PDT, and we believe that this effect if most likely additive. Moreover, we observed that the intracellular glutathione content was lower in KYSE170 cells, and the effect of SASP against glutathione was lower than that of BSO (Figs. 5B and 6B).

Although SASP enhanced the effect of VP-PDT *in vitro*, we did not investigate it *in vivo*, which is a limitation of this study. Therefore,

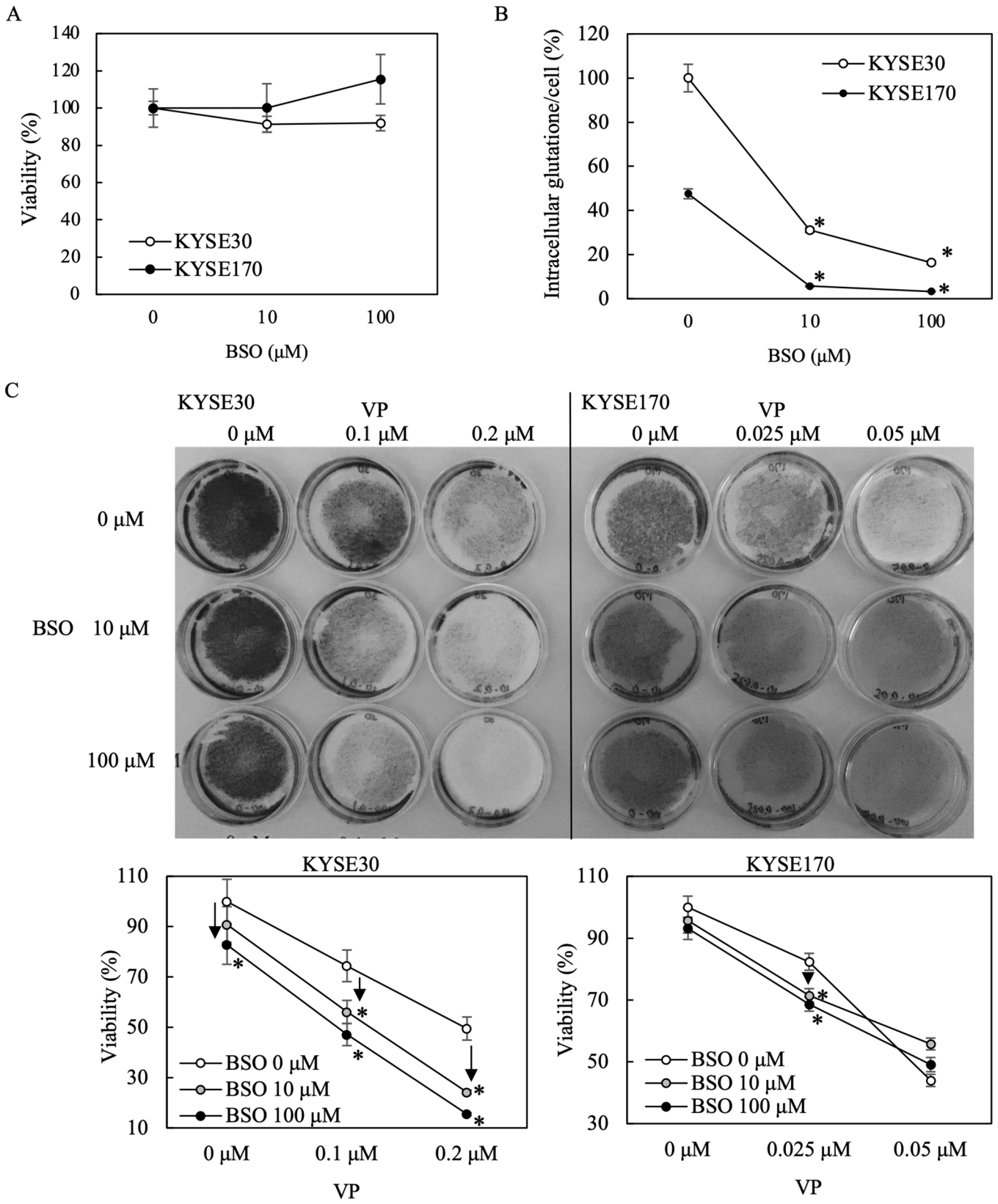

Fig. 5. Cytotoxic effects of BSO treatment on KYSE30 and KYSE170 cells. Cells were treated with BSO for 24 h. (A) Cytotoxicity was measured by the MTS assay. (B) The intracellular glutathione was measured by the GSH-Glo glutathione assay and corrected by the MTS assay. (C) The BSO treatment effect on VP-PDT. *$p < 0.05$ vs. each control ($n = 4$). The error bar indicates the standard deviation. BSO, L-Buthionine-(S, R)-sulfoximine for inhibiting glutathione synthesis. VP, verteporfin. PDT, photodynamic therapy.

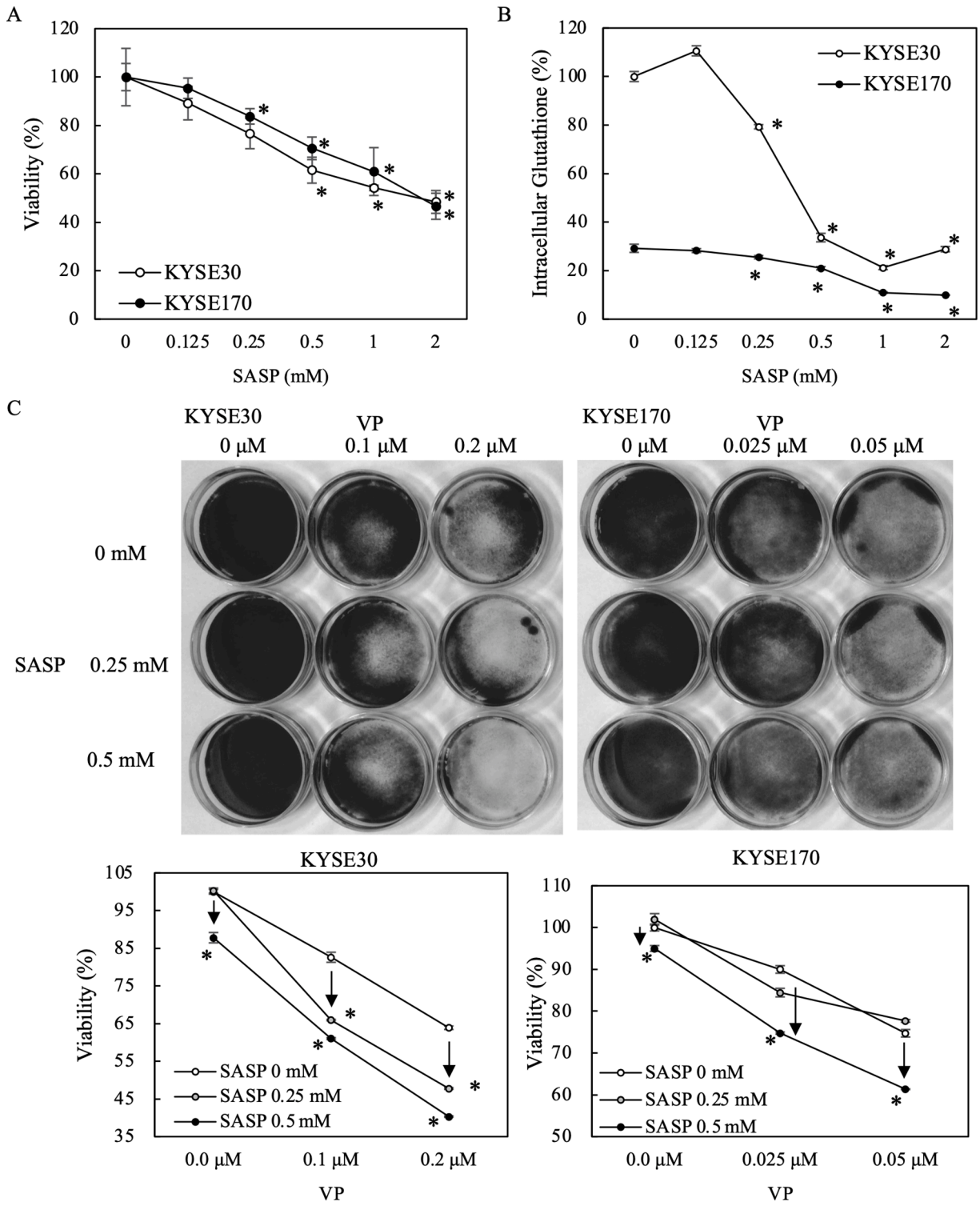

Fig. 6. Cytotoxic effects of SASP on KYSE30 and KYSE170 cells. Cells were treated with SASP for 24 h. (A) The cytotoxicity was measured by the MTS assay. (B) The intracellular glutathione was measured by the GSH-Glo glutathione assay and corrected by the MTS assay. (C) The effect on VP-PDT. *$p < 0.05$ vs. each control ($n = 4$). Error bars indicate the standard deviation. SASP, sulfasalazine. VP, verteporfin. PDT, photodynamic therapy.

investigations based on animal models and clinical studies are warranted in the future. However, it is noteworthy that SASP is already implemented in the clinic, but not for PDT, which is very promising in terms of drug repositioning.

Although VP is currently approved only for treating age-related macular degeneration, it can also be used to treat EC. In addition, VP is effective at lower concentrations than the TS concentration presently used to treat EC, suggesting that the treatment with lower VP concentrations may be more effective and safer, with fewer side effects, such as photosensitivity. In addition, the absorption peak of VP is at a longer wavelength than that of PS and TS and could reach deeper into tissues than visible light. Therefore, it could be used for treating deeper EC lesions. Nevertheless, side effects, such as hardening of the esophagus due to the deep light penetration of VP-PDT, are a subject for further

studies.

We used a 35 mm dish or a 96-well plate depending on whether cells were irradiated or not because there was unevenness of LED irradiation in this experiment. In addition, it was necessary to distinguish between the crystal violet and MTS assays owing to the cost of reagents and procedures. It is required to develop LEDs without uneven irradiation in the future.

This study has several limitations. First, it is necessary to use higher magnification when observing the localization of mitochondria. Second, it is necessary to analyze VP uptake using flow cytometry, which is a more quantitative approach.

PDT has been reported to be an effective treatment for chemotherapy and radiation-resistant cancers, causing direct damage to lipids and proteins and causing mitochondrial-induced apoptosis [15]. However, not all the mechanisms have been elucidated yet. Moreover, another photosensitizer, Tookad Soluble, treats prostate cancer by acting on the vascular system [16]. Therefore, it may be necessary to study VP-PDT in an experimental system that also contains blood vessels. However, it is complicated, different from the clinical system (because in the existing clinical system, there are EPR effects), and the actual effects can only be seen in humans. Therefore, in this study, we used a simple basic experimental system for verification.

In conclusion, the amount of intracellular glutathione critically affects VP-PDT efficacy, and SASP can boost the VP-PDT efficacy in EC treatment.

Acknowledgments

Not applicable.

Supplementary materials

Supplementary material associated with this article can be found, in the online version, at doi:10.1016/j.pdpdt.2022.103090.

References

[1] R.L. Siegel, K.D. Miller, A. Jemal, Cancer statistics, 2017, CA Cancer J. Clin. 69 (2017) 7–34, https://doi.org/10.3322/caac.21551.
[2] Y. Kitagawa, T. Uno, T. Oyama, K. Kato, H. Kato, H. Kawakubo, et al., Esophageal cancer practice guidelines 2017 edited by the Japan esophageal society: part 1, Esophagus 16 (2019) 1–24, https://doi.org/10.1007/s10388-018-0641-9.
[3] M. Ethirajan, Y. Chen, P. Joshi, R.K. Pandey, The role of porphyrin chemistry in tumor imaging and photodynamic therapy, Chem. Soc. Rev. 40 (2011) 340–362, https://doi.org/10.1039/b915149b.
[4] K.J. Messmer, S.R. Abel, Verteporfin for age-related macular degeneration, Ann. Pharmacother. 35 (2001) 1593–1598, https://doi.org/10.1345/aph.10365. Dec.
[5] M.T. Huggett, M. Jermyn, A. Gillams, R. Illing, S. Mosse, M. Novelli, et al., Phase I/II study of verteporfin photodynamic therapy in locally advanced pancreatic cancer, Br. J. Cancer 110 (2014) 1698–1704, https://doi.org/10.1038/bjc.2014.95.
[6] T. Kanda, T. Sugihara, T. Takata, Y. Mae, H. Kinoshita, T. Sakaguchi, et al., Low-density lipoprotein receptor expression is involved in the beneficial effect of photodynamic therapy using talaporfin sodium on gastric cancer cells, Oncol. Lett. 17 (2019) 3261–3266, https://doi.org/10.3892/ol.2019.10004.
[7] Y. Shibata, A. Matsumura, F. Yoshida, T. Yamamoto, K. Nakai, T. Nose, et al., Competitive uptake of porphyrin and LDL via the LDL receptor in glioma cell lines: flow cytometric analysis, Cancer Lett. 166 (2001) 79–87, https://doi.org/10.1016/S0304-3835(00)00717-5.
[8] E. Ogawa, S. Motohashi, A. Ito, T. Arai, Effects of albumin binding on photocytotoxicity of extracellular photosensitization reaction using talaporfin sodium to rat myocardial cells, Photodiagn. Photodyn. Ther. 12 (2015) 252–257, https://doi.org/10.1016/j.pdpdt.2015.02.001.
[9] H. Ito, H. Matsui, M. Tamura, H.J. Majima, H.P. Indo, I. Hyodo, Mitochondrial reactive oxygen species accelerate the expression of heme carrier protein 1 and enhance photodynamic cancer therapy effect, J. Clin. Biochem. Nutr. 56 (2015) 49–56, https://doi.org/10.3164/jcbn.14-27.
[10] T. Ishimoto, O. Nagano, T. Yae, M. Tamada, T. Motohara, H. Oshima, et al., CD44 variant regulates redox status in cancer cells by stabilizing the xCT subunit of system xc- and thereby promotes tumor growth, Cancer Cell 19 (2011) 387–400, https://doi.org/10.1016/j.ccr.2011.01.038.
[11] R. Seishima, K. Okabayashi, O. Nagano, H. Hasegawa, M. Tsuruta, M. Shimoda, et al., Sulfasalazine, a therapeutic agent for ulcerative colitis, inhibits the growth of CD44v9+cancer stem cells in ulcerative colitis-related cancer, Clin. Res. Hepatol. Gastroenterol. 40 (2016) 487–493, https://doi.org/10.1016/j.clinre.2015.11.007.
[12] L.A. Timmerman, T. Holton, M. Yuneva, R.J. Louie, M. Padró, A. Daemen, et al., Glutamine sensitivity analysis identifies the xCT antiporter as a common triple-negative breast tumor therapeutic target, Cancer Cell 24 (2013) 450–465, https://doi.org/10.1016/j.ccr.2013.08.020.
[13] K.J. Livak, T.D. Schmittgen, Analysis of relative gene expression data using real-time quantitative PCR and the 2-ΔΔCT method, Methods 25 (2001) 402–408, https://doi.org/10.1006/meth.2001.1262.
[14] Y. Mae, T. Kanda, T. Sugihara, T. Takata, H. Kinoshita, T. Sakaguchi, et al., Verteporfin-photodynamic therapy is effective on gastric cancer cells, Mol. Clin. Oncol. 13 (2020) 10, https://doi.org/10.3892/mco.2020.2081.
[15] S. Tangutoori, B.Q. Spring, Z. Mai, A. Palanisami, L.B. Mensah, T. Hasan, Simultaneous delivery of cytotoxic and biologic therapeutics using nanophotoactivatable liposomes enhances treatment efficacy in a mouse model of pancreatic cancer, Nanomedicine 12 (2016) 223–234, https://doi.org/10.1016/j.nano.2015.08.007.
[16] A.R. Azzouzi, E. Barret, C.M. Moore, A. Villers, C. Allen, A. Scherz, et al., TOOKAD® soluble vascular-targeted photodynamic (VTP) therapy: determination of optimal treatment conditions and assessment of effects in patients with localised prostate cancer, BJU Int. 112 (2013) 766–774, https://doi.org/10.1111/bju.12265.